

Strain relaxation in AlGa_xN/GaN superlattices grown on GaN

S. Einfeldt,^{a)} H. Heinke, V. Kirchner, and D. Hommel

Institute of Solid State Physics, University of Bremen, P.O. Box 330440, 28334 Bremen, Germany

(Received 17 July 2000; accepted for publication 20 November 2000)

Lattice relaxation of strained Al_xGa_{1-x}N/GaN superlattices grown on thick GaN buffer layers is investigated using optical microscopy, x-ray diffraction, and photoluminescence spectroscopy. The results are compared to strained bulk Al_xGa_{1-x}N layers particularly with regard to the impact of the superlattice period and the Al content. A relaxation process which keeps the coherency between Al_xGa_{1-x}N barriers and GaN wells in the superlattice is found and it is attributed to misfit dislocations at the buffer/superlattice interface. Additionally, the Al_xGa_{1-x}N barriers relax via crack channels which form beyond a critical Al content and limit the additional strain energy compared to a free-standing superlattice to a maximum value. Cracks relieve tensile plane stress to an extent similar as in bulk layers, i.e., they do not put the GaN wells of the superlattice under additional plane compression. This is explained by misfit dislocations which nucleate at crack faces and glide into the superlattice at the well/barrier interfaces. The onset of cracking is found to shift to higher tensile stresses in the Al_xGa_{1-x}N barriers when increasing the superlattice period which is discussed in view of edge cracks being the starting point of crack channels. © 2001 American Institute of Physics. [DOI: 10.1063/1.1342020]

I. INTRODUCTION

Extensive research activities have focused on the semiconductor alloy Al_xGa_{1-x}N during the last few years due to its application in devices as field effect transistors operating under high power or at high temperatures as well as laser diodes emitting in the blue and violet spectral region. In those structures, a high aluminum content is often favored in order to achieve either a two-dimensional electron gas of high concentration at Al_xGa_{1-x}N/GaN interfaces or a sufficient optical confinement for GaN waveguides embedded in Al_xGa_{1-x}N cladding layers. Two serious problems arise when the aluminum content is increased. First, Al_xGa_{1-x}N layers tend to crack since they are under high tensile stress when pseudomorphically grown on thick GaN buffers.¹ Second, *p*-type conductivity of Mg-doped Al_xGa_{1-x}N rapidly drops as the acceptor ionization energy increases.² Both issues significantly limit the opportunities to freely design device structures. One approach of resolution is to use short-period Al_xGa_{1-x}N/GaN superlattices (SLs) instead of Al_xGa_{1-x}N layers as was suggested and realized by Nakamura *et al.*^{3,4} Modulation doped SLs used as cladding layers in laser diodes were claimed to be tougher against cracking and to lower the threshold current density and voltage of laser operation.⁵ The latter fact was recently investigated in more detail by Kozodoy *et al.* who showed superior characteristics of the in-plane hole transport through Mg-doped SLs caused by pyroelectric and piezoelectric fields in the nitrides.^{6,7} However, clear experimental evidence for an improved cracking toughness of SLs compared to Al_xGa_{1-x}N epilayers is still missing.

The goal of this article is to investigate strain relaxation in Al_xGa_{1-x}N/GaN SLs which are grown on GaN. Recently,

we reported on the relief of tensile stress in single Al_xGa_{1-x}N layers on GaN.⁸ When ever possible the results on SLs presented here will be compared to those on Al_xGa_{1-x}N layers which in the following are termed bulk layers.

II. EXPERIMENT

Samples under investigation were grown by molecular beam epitaxy using a rf nitrogen plasma source. First, 1 μm of nominally undoped GaN was deposited as buffer on nitrated *c*-plane sapphire without previous nucleation layer, followed by the Al_xGa_{1-x}N SL with 1 μm overall thickness. The whole structure was grown at 820 °C under group-III rich growth conditions, which is favorable in view of a smooth epitaxial surface.⁹ Care was taken to maintain the same III/V flux ratio for the GaN well and the Al_xGa_{1-x}N barrier of the SL by rapidly changing the plasma power of the nitrogen source at each interface without growth interruption. Three series of samples with SL periods *t_p* of 5, 50, and 100 nm were produced, corresponding to 200, 20, and 10 period repetitions, respectively. Despite neglectable carrier confinement in the structures with periods of 50 and 100 nm, all the samples are termed SLs here to simplify matters. The well and barrier in each SL have nominally the same thickness and the Al content in the barrier was varied in each sample series with maximum values of about 0.65.

Sample surfaces were investigated by reflected light microscopy (RLM). Photoluminescence (PL) spectra were recorded at a temperature of 4 K using a HeCd laser operating at a wavelength of 325 nm as an excitation source. High resolution x-ray diffraction (XRD) was exploited to extract lattice parameters *c* and *a*, aluminum content, strain state of Al_xGa_{1-x}N and the SL period. This was achieved by performing triple-axis ω and 2θ-ω scans through (0002) reflec-

^{a)}Electronic mail: einfeldt@physik.uni-bremen.de

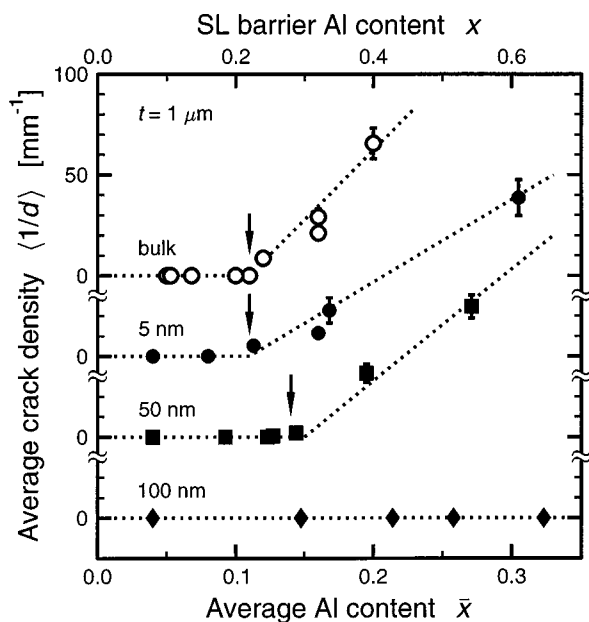


FIG. 1. Average crack density of $\text{Al}_x\text{Ga}_{1-x}\text{N}/\text{GaN}$ SLs of various periods (filled symbols) and bulk $\text{Al}_x\text{Ga}_{1-x}\text{N}$ layers (open circles) vs Al content. The data points for different sample series are vertically shifted for reasons of clearness. The dotted lines are guides to the eye, and the arrows mark the onset of cracking.

tions of GaN and $\text{Al}_x\text{Ga}_{1-x}\text{N}$ the latter one exhibiting satellites from the periodic SL structure. The extracted period was found to coincide with the intended values within 5%. Moreover, reciprocal space maps for the $(10\bar{1}5)$ reflection were recorded and evaluated, as described in Ref. 10, to determine the extent of biaxial tensile strain of $\text{Al}_x\text{Ga}_{1-x}\text{N}$ relative to GaN given by the strain parameter γ . The latter parameter changes linearly with strain: It is one for the pseudomorphic case and zero for the fully relaxed case. As in our previous work,⁸ the stiffness constants c_{ij} published by Wright *et al.*¹¹ are used throughout this article, particularly also to calculate the two-dimensional Poisson ratio $\nu_c = -2c_{13}/c_{33} = -0.51$ which connects in-plane strain $\Delta a/a$ and out-of-plane strain $\Delta c/c$.

III. RESULTS AND DISCUSSION

A. Stress relieving mechanisms

Crack channels are observed on various SL samples whose appearance is very similar to those on bulk layers.⁸ They run along $\langle 2110 \rangle$, are similarly dense for all three equivalent crystal directions, and usually terminate at other cracks crossing their pathway. In contrast to bulk layers, delamination of SLs from the GaN buffer was not observed even for the highest Al contents used in this work. The extent of cracking can be described by the average crack density, i.e., the inverse intercrack spacing measured perpendicular to the direction of crack channels at various points on the sample. The results of corresponding RLM observations are summarized in Fig. 1. SLs with a period of 5 nm start to crack at a barrier Al content of $x = 0.22$ which is similar to bulk layers when taking the average Al content \bar{x} (in our case half the barrier Al content x) as reference. Beyond this value,

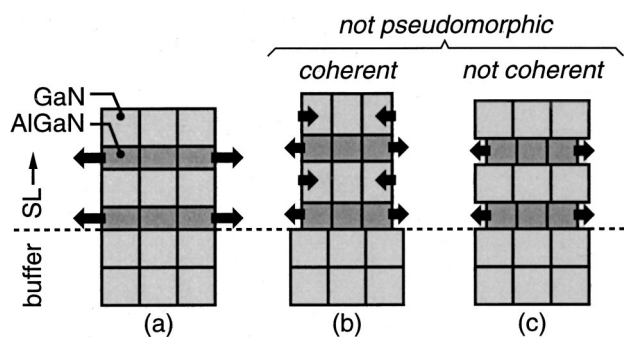


FIG. 2. Schematic illustration of the different modes of stress relief of a coherent $\text{Al}_x\text{Ga}_{1-x}\text{N}/\text{GaN}$ SL which is pseudomorphic to a GaN buffer as shown in (a): Termination of the pseudomorphy only by relaxation of the whole SL against the buffer (b) and termination of the coherency within the SL by isolated relaxation of the wells against the barriers (c). Arrows mark the normal in-plane stress of the layers.

the crack density gradually increases. Thus, short-period SLs behave like an effective alloy formed by intermixing wells and barriers. On the other hand, SLs with a period of 50 nm show slightly delayed cracking with a critical Al content of $x = 0.28$. None of the SLs with a 100 nm period exhibited cracks despite high Al contents of more than 0.6 in the barriers.

Discussing the stress relief in SLs, one has to distinguish two fundamental mechanisms which are schematically shown in Fig. 2. Before any relaxation starts, the SL is coherent, i.e., $\text{Al}_x\text{Ga}_{1-x}\text{N}$ barrier and GaN well have the same in-plane lattice parameter. Since the SL is pseudomorphically grown on a relaxed GaN buffer, only the barriers are under tensile plane stress as illustrated in Fig. 2(a). Terminating the pseudomorphy but keeping the SL coherent as shown in Fig. 2(b) relieves tensile stress in $\text{Al}_x\text{Ga}_{1-x}\text{N}$ but, in parallel, builds up compressive plane stress in the GaN wells. This process is a relaxation mechanism as it reduces the overall strain energy which quadratically depends on the strain. Alternatively, tensile stress in the SL barriers can be relieved independently from the adjacent wells as shown in Fig. 2(c), which terminates the coherency of the SL.

A relaxation process similar to that illustrated in Fig. 2(c) was theoretically investigated by Bykhovski *et al.*,¹² who balanced the formation energy of misfit dislocations at the various well/barrier interfaces in the SL with the connected reduction in strain energy to derive critical thicknesses and Al contents. It should be noted that these authors considered free-standing SLs which are not forced to be pseudomorphic to a buffer as in Fig. 2(a), i.e., overall stress is shared between $\text{Al}_x\text{Ga}_{1-x}\text{N}$ barrier and GaN well for the nonrelaxed case. Their results are shown as the solid curve in Fig. 3(a) together with our experimental data for SLs with periods of 5 and 50 nm as well as data taken from the literature.^{4,5,13–18} Whether the coherency state (squares) or the cracking state (circles) were used to characterize the samples listed in Fig. 3 depends on the information given in the corresponding publications. Moreover, cracked samples are not included in Fig. 3(a) as it is aimed to illustrate coherency rather than pseudomorphy. Obviously, the theory of Bykhovski *et al.*¹² is supported by the experiments although

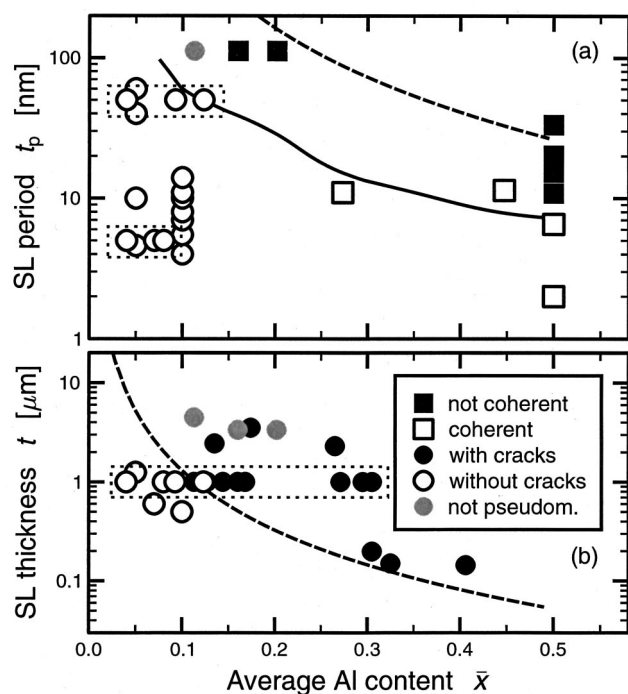


FIG. 3. Strain state of $\text{Al}_x\text{Ga}_{1-x}\text{N}/\text{GaN}$ SLs of different average Al content, period (a) and overall thickness (b). Both our own data (symbols framed by dotted boxes) and those found in the literature are included. Coherent SLs ($a_{\text{SL}}^{\text{AlGa}} = a_{\text{GaN}}^{\text{SL}}$) are marked by open squares whereas filled squares are used for not coherent ones ($a_{\text{SL}}^{\text{AlGa}} < a_{\text{GaN}}^{\text{SL}}$). SLs reported to be either cracked or free of cracks are shown by open or black filled circles, respectively. Gray circles stay for SLs which are not pseudomorphic to the buffer ($a_{\text{SL}}^{\text{AlGa}} < a_{\text{GaN}}^{\text{buffer}}$). The solid curve in (a) is taken from Ref. 12 and marks the expected onset of relaxation in a free-standing SL by the formation of misfit dislocations. The dashed curves correspond to the onset of crack channeling as discussed in Ref. 8 using a fracture toughness of 9 J/m^2 . Cracking of an individual $\text{Al}_x\text{Ga}_{1-x}\text{N}$ barrier (a) or cracking of the whole SL by considering it as a bulk layer with the same average Al content (b) were assumed.

additional experimental data are needed for a more reliable statement. The agreement is to some extent surprising since the calculations are based on a thermodynamic approach which does not consider the formation process of misfit dislocations. The latter one is often assumed to consist of bending and gliding of pre-existing threading dislocations as suggested by Matthews and Blakeslee.¹⁹ However, due to high Peierls forces in wurtzite nitrides, dislocation gliding is unlikely to occur as was recently claimed by Jahnen *et al.*²⁰ Therefore, relaxation may start only at higher stresses than those calculated by Bykhovski *et al.*¹² On the other hand, Jahnen *et al.*²⁰ found that in compressively strained $\text{In}_x\text{Ga}_{1-x}\text{N}$ on GaN misfit dislocations can form via V-shaped pinholes. Consequently, one may speculate that in $\text{Al}_x\text{Ga}_{1-x}\text{N}$ a similar role is overtaken by the commonly observed cracks. Indeed, this is supported by recent experiments of Hearne *et al.*²¹ on bulk $\text{Al}_x\text{Ga}_{1-x}\text{N}$ layers. All SLs which so far have been reported to be not coherent^{13,14,16} have such large overall thicknesses, that bulk layers with the same average Al content are expected to crack.⁸ Unfortunately, cracking in these SLs has not been discussed.

To find out which of the two stress relieving mechanisms shown in Figs. 2(b) and 2(c) dominates in our SLs, the

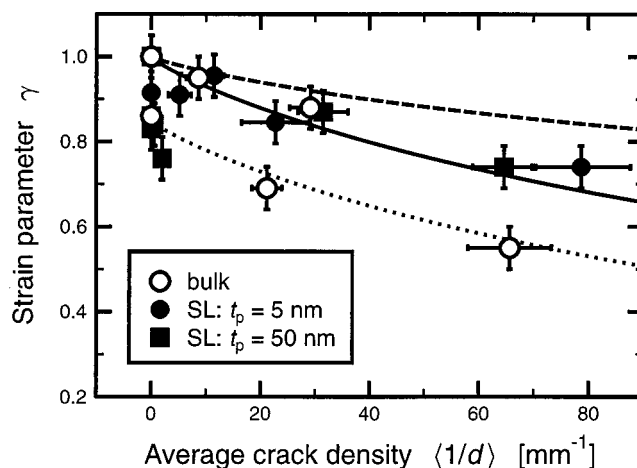


FIG. 4. Strain parameter of $\text{Al}_x\text{Ga}_{1-x}\text{N}$ relative to the GaN buffer for $\text{Al}_x\text{Ga}_{1-x}\text{N}/\text{GaN}$ SLs (filled symbols) and bulk $\text{Al}_x\text{Ga}_{1-x}\text{N}$ layers (open circles) vs average crack density. The lines correspond to the theoretical expectations based on the model of an isolated stripe film on a substrate for the case of bulk layers (γ , solid line), bulk layers with an additional relaxation mechanism ($\gamma - 0.15$, dotted line), and SLs ($1/2 + \gamma/2$, dashed line).

strain parameter γ was determined by XRD for all samples. In this case, the parameter describes the relative strain of the $\text{Al}_x\text{Ga}_{1-x}\text{N}$ SL barrier compared to the GaN buffer layer. In Fig. 4, the strain parameters are plotted versus the average crack density. Obviously, SLs behave like bulk layers which can be divided into two groups separated by $\Delta\gamma = -0.15$ whose strain parameters decrease with the crack density. A quantitative description of strain relaxation by cracks can be given when considering the area between two crack channels as an isolated stripe film on a substrate. Corresponding stress distributions were derived by Atkinson *et al.*²² which are applied to our experimental data by assuming XRD to reflect the average strain between two crack channels (see Ref. 8 for more details). The solid line in Fig. 4 is the outcome of this model applied to bulk layers which fits to all data when shifted by $\Delta\gamma = -0.15$ (dotted line) for the second set of samples. Consequently, bulk layers relax via the formation of cracks and an additional mechanism of unknown origin inducing the drop by $\Delta\gamma$. It is remarkable that the SLs show exactly the same behavior. Relaxation of SLs by cracks only corresponds to Fig. 2(b). In this case, γ should decrease with the crack density only half as strongly as in the case of bulk layers because the final relaxation state is a free-standing SL with $\gamma = 0.5$ for the case that well and barrier have the same thickness and elastic properties, instead of $\gamma = 0$ for bulk layers. Therefore, SLs should rather lie on the dashed curve in Fig. 4.

In conclusion of Fig. 4, cracking is involved in strain relaxation of SLs as the strain of the $\text{Al}_x\text{Ga}_{1-x}\text{N}$ barriers smoothly depends on the crack density. However, since the degree of relaxation rather fits to the expectations for bulk layers, relaxation is not significantly limited by the formation of compressive plane stress in the GaN wells. In other words, with the formation of cracks, another mechanism is postulated which allows the wells to relieve part of the induced stress. This idea is supported by PL measurements which will be discussed later.

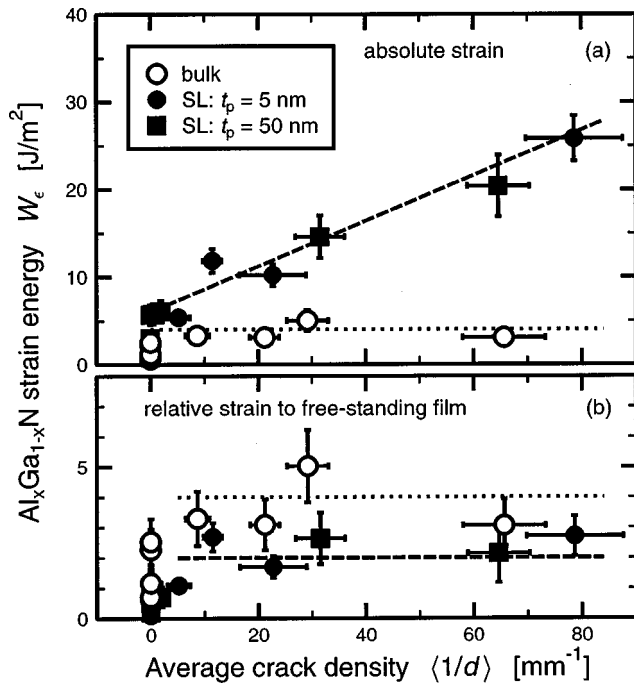


FIG. 5. Strain energy of $\text{Al}_x\text{Ga}_{1-x}\text{N}$ per film area vs average crack density. The absolute strain (a) or the relative strain compared to a free-standing film not pseudomorphic to a GaN buffer (b) are used. The broken lines are guides to the eye.

In Fig. 5, the average strain energy W_e of $\text{Al}_x\text{Ga}_{1-x}\text{N}$ per unit area of the stressed films is shown in dependence on the average crack density. For a film of thickness t under plane stress, this energy is given in terms of the in-plane isotropic strain ϵ by

$$W_e = (c_{11} + c_{12} - 2c_{13}^2/c_{33})\epsilon^2 t. \quad (1)$$

Using the absolute strain of $\text{Al}_x\text{Ga}_{1-x}\text{N}$ given by $\epsilon(x) = \gamma\epsilon_0(x)$ with $\epsilon_0(x)$ as the in-plane coherency strain to GaN, the values plotted in Fig. 5(a) were derived. As was already pointed out in Ref. 8, the strain energy of bulk layers saturates at a maximum value of about 4 J/m^2 which is in line with the common idea in fracture mechanics that fracture toughness can be described by a critical strain energy. For SLs however, the energy increases linearly with the crack density. Moreover, it is higher than that for bulk layers although the thickness t used in Eq. (1) for SLs is only half the value for bulk layers, as half of each SL consists of GaN the strain of which is not considered in Fig. 5(a). In explanation of these findings, one has to recall that stress relief in a SL by cracking should leave the well and barrier coherent as shown in Fig. 2(b). Therefore, in contrast to bulk layers even for extended cracking, the strain energy will not tend to zero. This can be taken into account by only considering the relative strain of $\text{Al}_x\text{Ga}_{1-x}\text{N}$ compared to a free-standing film as only this one can relax by cracks. For a SL in which the well and barrier have the same thickness and identical elastic constants, we have to apply $\epsilon(x) = (2\gamma - 1)\epsilon_0(x)/2$ because maximum relaxation is achieved by $\epsilon(x) = \epsilon_0(x)/2$ or $\gamma = 0.5$. The corresponding strain energy is shown in Fig. 5(b). Now, SLs exhibit a saturation behavior similar to bulk layers but at about half the strain energy value. This does not

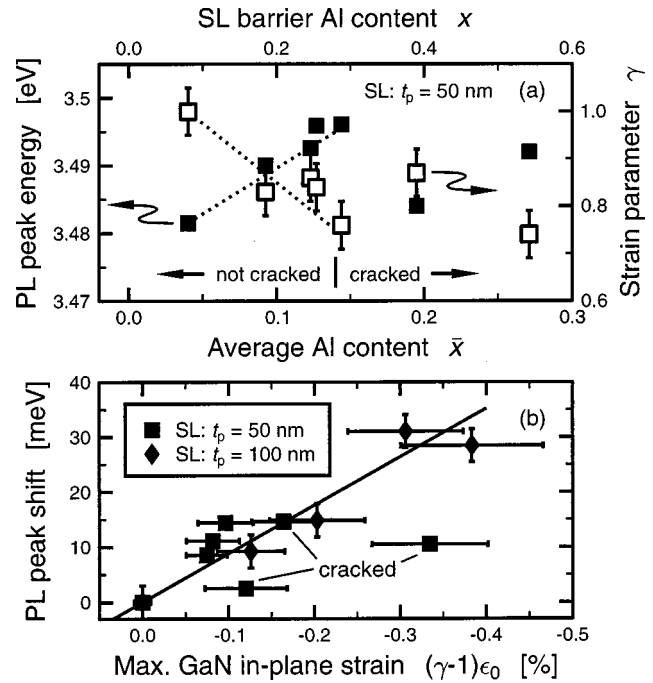


FIG. 6. (a) D^0X peak position in PL spectra taken at 4 K (filled squares) and strain parameter (open squares) vs Al content of SLs with a period of 50 nm. The dotted lines are guides to the eye. (b) Spectral shift of D^0X peaks at 4 K for SLs with periods of 50 nm (squares) and 100 nm (diamonds), respectively, vs maximum in-plane strain of GaN wells. The latter one was calculated from the strain parameter of the $\text{Al}_x\text{Ga}_{1-x}\text{N}$ barriers by assuming the wells to be coherent to the barriers. The solid line corresponds to the theoretical expectation for GaN under plane stress using an effective deformation potential of $\bar{D} = -8.8 \text{ eV}$.

indicate a lower fracture toughness of SLs since the $\text{Al}_x\text{Ga}_{1-x}\text{N}$ volume portion of those films is only one half. Strictly speaking, the energy contribution from the wells should be considered for the SLs in Fig. 5(b), as well. However, the strain of the wells can not be easily extracted from the XRD measurements.

A very direct method to determine the strain state of the GaN wells in the SLs is to measure the GaN band gap which should increase with the compressive strain in the c -plane. SLs with wide wells are well suited for this experimental approach because quantization effects due to the confinement of carriers in the wells can be nearly neglected such that PL spectra directly provide the band gap of GaN. In contrast, evaluation of the PL of short-period SLs would require miniband calculations under consideration of piezoelectric and pyroelectric fields which is beyond the scope of this work. In Fig. 6(a), the positions of the highest-energetic peak in the PL spectra are summarized for SLs with a period of 50 nm. The peak, which is assumed to correspond to the recombination of excitons bound to neutral native donors (D^0X) in the GaN wells, continuously shifts to higher energies with an increasing Al content for noncracked samples, i.e., the GaN wells become more compressively strained. In parallel, the strain parameter decreases from 1 to about 0.75 showing the $\text{Al}_x\text{Ga}_{1-x}\text{N}$ barriers to relieve tensile stress. It should be emphasized that both phenomena are observed at SLs on which no cracks could be found. Moreover, in this case, relaxation starts at Al contents below the critical value for the forma-

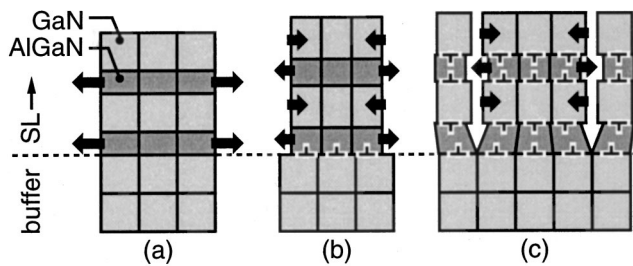


FIG. 7. Proposed steps of stress relief of strained $\text{Al}_x\text{Ga}_{1-x}\text{N}/\text{GaN}$ SLs pseudomorph on a GaN buffer as shown in (a). First, dislocations form at the buffer/SL interface terminating the pseudomorphy but keeping the coherency of the SL (b). Second, the SL cracks and dislocations form at the $\text{Al}_x\text{Ga}_{1-x}\text{N}/\text{GaN}$ interfaces in the SL, which terminates its coherency (c). Arrows mark the normal in-plane stress of the layers.

tion of misfit dislocations within the SL, which is about $\bar{\epsilon} = 0.12$ for a period of 50 nm when referring to the calculations of Bykhovski *et al.*¹²

The PL data can be quantitatively explained by assuming a relaxation mechanism other than cracking which keeps the coherency of the SL but terminates the pseudomorphy of the SL to the GaN buffer as shown in Fig. 2(b). In this case, the stress relieved by the $\text{Al}_x\text{Ga}_{1-x}\text{N}$ barriers should be completely accommodated by the GaN wells, whose biaxial compressive strain is then given by $\epsilon(x) = (\gamma - 1)\epsilon_0(x)$. The accompanied spectral blueshift ΔE of the GaN band gap can be calculated by²³

$$\Delta E = [\nu_c(D_1 + D_3) + 2(D_2 + D_4)]\epsilon = \bar{D}\epsilon, \quad (2)$$

where D_i are the relevant deformation potentials for wurtzite GaN. Various values have been published for the latter parameters resulting in \bar{D} values in the range of -7.28 to -12.2 eV.^{24–30} The dependence of Eq. (2) is shown as the line in Fig. 6(b) for an average \bar{D} value of -8.8 eV together with our experimental data both for the SLs with a 50 nm as well as a 100 nm period. Experiment and theory fit quite well for the noncracked samples. It should be noted that the experimentally observed blueshift of the PL would be smaller if the SLs were not coherent. Seeking a microscopic process which builds up the strain in the GaN wells, the formation of misfit dislocations at the SL/buffer interface, as shown in Fig. 7(b), seems to be most probable. In terms of strain energy release, this interface is preferred for dislocations as tensile stress of the whole SL can be relieved.

Discussing the strain of GaN wells in cracked SLs, the termination of the PL blueshift, as shown in Fig. 6(a), has to be explained. If cracking is a relaxation mechanism, as shown in Fig. 2(b), then cracks should induce additional compressive plane stress in GaN, i.e., the PL blueshift should proceed. The fact that this is not observed points to an additional relaxation mechanism closely related to the formation of cracks which avoids GaN to become further stressed. The formation of misfit dislocations at the $\text{Al}_x\text{Ga}_{1-x}\text{N}/\text{GaN}$ interfaces in the SL, as shown in Fig. 7(c), is suggested. This process is induced by cracks whose faces provide the needed nucleation sites for dislocations which then glide in the c -plane into the SL. As previously mentioned, a similar mechanism was reported by Hearne *et al.*²¹ for bulk $\text{Al}_x\text{Ga}_{1-x}\text{N}$

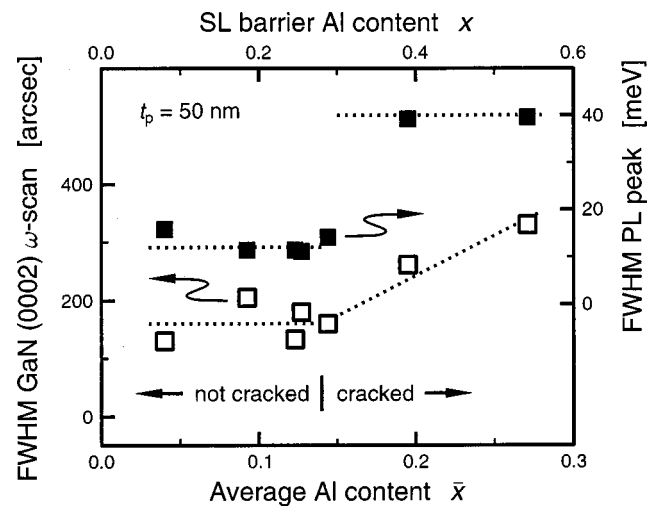


FIG. 8. Full width at half maximum (FWHM) of rocking curves corresponding to the (0002) reflection of GaN (open symbols) and FWHM of D^0X peak in PL spectra taken at 4 K (filled symbols) vs Al content of SLs with a period of 50 nm. Dotted lines are guides to the eye.

layers on GaN. Also, the proposed scenario is consistent with the results shown in Fig. 4, for which it was stated that the stress relief via cracks in the SLs rather fits to the expectations for bulk layers: Due to simultaneous formation of misfit dislocations within the SL, the $\text{Al}_x\text{Ga}_{1-x}\text{N}$ barriers are not hindered by the GaN wells to relax and they behave like bulk layers. Moreover, the classification of both bulk layers and SLs into two groups differing in strain parameter by $\Delta\gamma = -0.15$ can be attributed to the occurrence or nonoccurrence of misfit dislocations at the buffer interface as shown in Fig. 7(b) before cracking starts. That dislocations form in the SLs also fits to the evolution of half widths of the PL peak and the XRD rocking curve corresponding to the (0002) reflection of GaN. Both parameters increase for cracked samples as shown in Fig. 8. However, the inhomogeneous stress distribution in cracked samples should have a similar impact as well.

B. Fracture toughness

Experimental data has yet to demonstrate that $\text{Al}_x\text{Ga}_{1-x}\text{N}/\text{GaN}$ SLs may effectively suppress cracking in comparison to bulk $\text{Al}_x\text{Ga}_{1-x}\text{N}$ layers of the same average Al content as proposed by Nakamura *et al.*^{3,4} The average Al content in $0.6 \mu\text{m}$ thick SLs, which were used by the latter authors as cladding layers in laser diodes, was $\bar{x} = 0.07$. On the other side, in former reports on bulk cladding layers of the same thickness, the Al content was given as $x = 0.08$.³¹ Hansen *et al.* who work on similar devices, reported on $0.5 \mu\text{m}$ thick cladding layers with $\bar{x} = 0.1$ layed out either as bulk or as SL.⁵ Few publications claim the realization of crack-free SLs of even high Al contents,^{32,33} which however required special growth procedures for the GaN buffer layer to keep its thickness or structural quality sufficiently low. Therefore, those SLs are expected to not grow pseudomorphically thereon but relieve stress by defects others than cracks, which are most probably misfit dislocations.

Stress relief by cracks was extensively discussed for bulk layers in our previous publication.⁸ The corresponding approaches should now be extended to SLs in order to interpret their cracking behavior shown in Fig. 1. Cracking of bulk layers in the composition range $0 < x < 0.2$ can be described by applying a constant fracture toughness of $\Gamma = 9 \text{ J/m}^2$ to the steady-state strain energy release rate $G_{ss}^{\text{bulk}}(x, t)$ per unit length of the front of a crack channeling across the $\text{Al}_x\text{Ga}_{1-x}\text{N}$ film³⁴

$$\Gamma = G_{ss}^{\text{bulk}}(x, t) = 1.976\sigma_0(x)^2 t / \bar{E}(x). \quad (3)$$

Here $\bar{E}(x) = E(x)/(1 - \nu(x)^2)$ with E as Young's modulus and ν as the Poisson ratio. In Ref. 8, the constant values $E = 306 \text{ GPa}$ and $\nu = 0.203$ of GaN were applied to both layer and substrate. $\sigma_0(x)$ is the normal in-plane stress of the layer for the pseudomorphic case. The latter one is given by

$$\sigma_0(x) = \left(c_{11}(x) + c_{12}(x) - 2 \frac{c_{13}(x)^2}{c_{33}(x)} \right) \epsilon_0(x). \quad (4)$$

In the case of a SL, one has to consider that the tensile stress $\sigma_0(x)$ in the $\text{Al}_x\text{Ga}_{1-x}\text{N}$ barriers is not completely relieved at the crack faces but only down to an intermediate value $\sigma_{\text{AlGa}}^{\text{SL}}(x)$ since in parallel, a compressive stress $\sigma_{\text{GaN}}^{\text{SL}}(x)$ is built up in the GaN wells. Those two stresses correspond to the equilibrium state in a free-standing SL. The energy release rate for crack channeling through a SL should thus be written

$$G_{ss}^{\text{SL}}(x, t) = 1.976t/2 \left(\frac{\sigma_0(x)^2 - \sigma_{\text{AlGa}}^{\text{SL}}(x)^2}{\bar{E}(x)} - \frac{\sigma_{\text{GaN}}^{\text{SL}}(x)^2}{\bar{E}(0)} \right). \quad (5)$$

The prefactor 1/2 results from the fact that the SL consists of half $\text{Al}_x\text{Ga}_{1-x}\text{N}$ and half GaN. Neglecting the composition dependence of the elastic constants, one obtains $\sigma_{\text{AlGa}}^{\text{SL}}(x) = -\sigma_{\text{GaN}}^{\text{SL}}(x) = \sigma_0(x)/2$ and $G_{ss}^{\text{SL}}(x, t) = G_{ss}^{\text{bulk}}(x/2, t)$. Consequently, the critical parameters for cracking should not differ between SLs and bulk layers of the same average Al content. Referring to Fig. 1, this is at least the case for short-period SLs which start to crack at $\bar{x} = 0.11$ similar to bulk layers. Moreover, the cracking state of all SLs reported,^{15,16,32,33,35} as summarized in Fig. 3(b), is in line with the critical curve for cracking of $\text{Al}_x\text{Ga}_{1-x}\text{N}$ bulk layers derived from Eq. (3). However, the long-period SLs presented in Fig. 1 exhibit a clearly different cracking behavior. It should be once more emphasized that the SLs with a period of 100 nm, which did not crack at all, have not been included in Fig. 1. Several aspects of cracking will now be discussed to explain why certain SLs could be tougher than bulk layers.

(i) Giving up the approximation of composition independent elastic properties as AlN is obviously stiffer than GaN, the strain energy change due to cracking should be smaller in the $\text{Al}_x\text{Ga}_{1-x}\text{N}$ barriers than in the GaN wells. This fact reduces the overall energy release rate and makes SLs tougher than bulk layers. To quantify this the stiffness constants of GaN and AlN were taken from Ref. 11 and linearly interpolated for $\text{Al}_x\text{Ga}_{1-x}\text{N}$. Then, the stresses $\sigma_{\text{AlGa}}^{\text{SL}}(x)$ and $\sigma_{\text{GaN}}^{\text{SL}}(x)$ were calculated by minimizing the overall

strain energy in a free-standing SL and inserted in Eq. (5). It turned out that the strain energy release rates of bulk layers and SLs differ by less than 1% for $\bar{x} = 0.10 - 0.15$. Assuming the fracture toughness to only linearly depend on the composition, this can be translated into critical Al contents for cracking: If the latter one is 0.11 for bulk layers as shown in Fig. 1, we expect SLs of the same thickness to crack at an average Al content which is only by 0.0004 higher than this. This is by far less than observed for SLs with longer periods (compare Fig. 1).

(ii) Instead of considering crack propagation, toughness can also be discussed in terms of crack nucleation. In the first stage, edge cracks are assumed to nucleate around flaws at the free sample surface which then propagate towards the GaN buffer. Only in the second step does crack channeling start.⁸ For bulk layers, the strain energy release rate of edge cracks linearly increases with the crack depth when film and substrate have identical elastic constants.³⁴ In contrast, edge cracks propagating through a SL have to pass the unstressed or even compressively stressed GaN wells. In this region, the energy release rate should drop rapidly.³⁶ Thus, the formation of extended edge cracks as a prerequisite for crack channeling might be impeded in SLs. According to this model, the cracking toughness of SLs should increase with their period, i.e., with increased thickness of the GaN wells, as shown in Fig. 1.

(iii) The formation of cracks requires the existence of flaws in the material because those serve as nucleation sites for cracks. Threading dislocations with a Burgers vector component along the c -axis are reported to partially bend and annihilate each other at $\text{Al}_x\text{Ga}_{1-x}\text{N}/\text{GaN}$ interfaces resulting in layers with significantly reduced defect densities.³⁷ If those dislocations contribute to crack nucleation, SLs can be expected to crack more difficult. Figure 9 presents half widths of rocking curves for the (0002) reflection since the latter one is sensitive to the dislocations of interest. The density of the dislocations in the SL increases with the Al content without any significant relation to the SL period.

(iv) As was discussed earlier, crack-free SLs are not always pseudomorphic to the GaN buffer since misfit dislocations are supposed to form at the buffer/SL interface as sketched in Fig. 7(b). The amount of stress which is not relieved by the dislocations will determine the onset of cracking. Therefore, one could attribute the difference in fracture toughnesses between SLs of different periods to a varying density of those dislocations. However, the strain parameter of all SLs equally decreases with increasing Al content. Particularly, the SLs with a period of 100 nm, on which cracks were not observed at all, do not exhibit extraordinary small strain parameters.

(v) In SLs with a period of 100 nm, cracking of the individual $\text{Al}_x\text{Ga}_{1-x}\text{N}$ barriers is expected for $x > 0.51$ when referring to the dashed curve in Fig. 3(a). Therefore, cracks may have already formed during growth of the very first barrier which were then overgrown and are thus not detectable with RLM. On the other hand, those cracks should not form as long as $x < 0.51$ which, however, is a composition range where the cracking behavior of SLs with 100 nm pe-

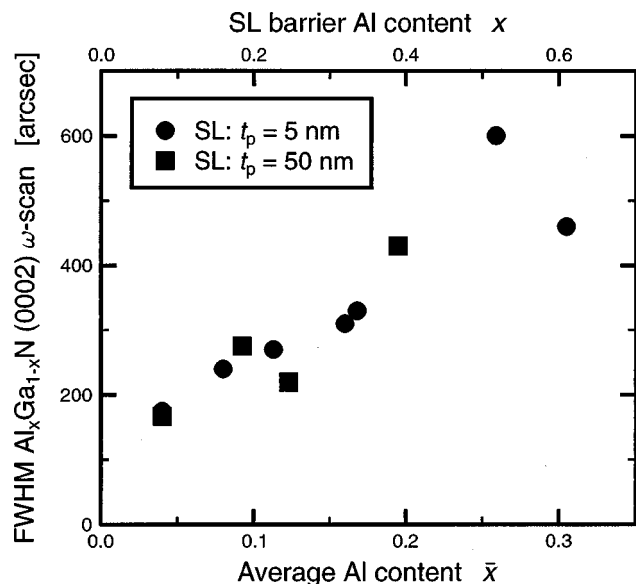


FIG. 9. FWHM of rocking curves corresponding to the (0002) reflection of $\text{Al}_x\text{Ga}_{1-x}\text{N}$ vs Al content of SLs with a period of 5 nm (●) and 50 nm (■), respectively.

riod also significantly deviates from that of other SLs with shorter periods.

In conclusion of items (i) to (v), it seems most likely that the suppressed formation of extended edge cracks, as discussed in (ii), is responsible for the increased fracture toughness of SLs with long periods. As a consequence, nitride based laser diodes should not significantly benefit from the use of short-period $\text{Al}_x\text{Ga}_{1-x}\text{N}/\text{GaN}$ SLs instead of bulk $\text{Al}_x\text{Ga}_{1-x}\text{N}$ as cladding layers in view of their cracking resistance. Due to the advantageous change in the characteristics of carrier transport, SLs should, nevertheless, be preferred in these devices compared to bulk layers.⁵⁻⁷

IV. SUMMARY

The relaxation of strained $\text{Al}_x\text{Ga}_{1-x}\text{N}/\text{GaN}$ SLs which are pseudomorphic to GaN buffer layers can be comprehensively explained by an interplay of misfit dislocations at various interfaces and extended crack channels along $\langle 2\bar{1}10 \rangle$ through the film. Below a critical Al content, which is about 0.22 and 0.28 for 1 μm thick SLs with periods of 5 nm and 50 nm, respectively, cracks do not form and the SL remains coherent, i.e., well and barrier are fully strained against each other. In those SLs, tensile plane stress of the $\text{Al}_x\text{Ga}_{1-x}\text{N}$ barriers can be partially relieved by misfit dislocations at the SL/buffer interface which simultaneously put the GaN wells under plane compression. This becomes apparent in a blue-shift of the GaN band gap which can be quantitatively described by published deformation potentials. As soon as cracks form, stress in the SLs is further relieved and the excess strain energy compared to a free-standing SL levels off at a maximum value of about 2 J/m^2 . The extent of relaxation can be well described by theoretical stress distributions between two neighboring crack channels. Since cracks in SLs reduce stress similar as in bulk layers, it is suggested that cracks act as nucleation sites for misfit dislocations at

the well/barrier interfaces which prevent the GaN wells to become further compressively stressed by cracks. This is confirmed by the fact that in cracked SLs the band gap of the GaN wells stops to shift blue. The fracture toughness for the onset of crack channeling through the film as measured by the critical Al content is found to be similar for bulk layers and short-period SLs but to increase significantly with the SL period. This can be most convincingly explained by the difficulty to form edge cracks through the whole SL including the compressively strained GaN wells which is the prerequisite for crack channeling.

ACKNOWLEDGMENTS

The authors would like to thank S. Hesselmann for sample preparation, K.-H. Vennen-Damm for maintaining the molecular-beam epitaxy system, and S. Neumann and L. Menzel for performing PL measurements. The work was partially supported by the Volkswagen Foundation under Contract No. I/74 452.

- ¹K. Itoh, K. Hiramatsu, H. Amano, and I. Akasaki, *J. Cryst. Growth* **104**, 533 (1990).
- ²M. Suzuki, J. Nishio, M. Onomura, and C. Hongo, *J. Cryst. Growth* **189**, 511 (1998).
- ³S. Nakamura *et al.*, *Jpn. J. Appl. Phys., Part 2* **36**, L1568 (1997).
- ⁴S. Nakamura *et al.*, *Appl. Phys. Lett.* **72**, 211 (1998).
- ⁵M. Hansen *et al.*, *Phys. Status Solidi A* **176**, 59 (1999).
- ⁶P. Kozodoy, M. Hansen, S. P. DenBaars, and U. K. Mishra, *Appl. Phys. Lett.* **74**, 3681 (1999).
- ⁷P. Kozodoy *et al.*, *Appl. Phys. Lett.* **75**, 2444 (1999).
- ⁸S. Einfeldt, V. Kirchner, H. Heinke, M. Dießelberg, S. Figge, K. Vogeler, and D. Hommel, *J. Appl. Phys.* **88**, 7029 (2000).
- ⁹E. J. Tarsa, B. Heying, X. H. Wu, P. Fini, S. P. DenBaars, and J. S. Speck, *J. Appl. Phys.* **82**, 5472 (1997).
- ¹⁰H. Heinke, M. O. Möller, D. Hommel, and G. Landwehr, *J. Cryst. Growth* **135**, 41 (1994).
- ¹¹A. Wright, *J. Appl. Phys.* **82**, 2833 (1997).
- ¹²A. D. Bykhovskii, B. L. Gelmont, and M. S. Shur, *J. Appl. Phys.* **81**, 6332 (1997).
- ¹³Z. Sitar, M. J. Paisley, B. Yan, J. Ruan, W. J. Choyke, and R. F. Davis, *J. Vac. Sci. Technol. B* **8**, 316 (1990).
- ¹⁴Z. Sitar, M. J. Paisley, B. Yan, R. F. Davis, J. Ruan, and J. W. Choyke, *Thin Solid Films* **200**, 311 (1991).
- ¹⁵K. Itoh, T. Kawamoto, H. Amano, K. Hiramatsu, and I. Akasaki, *Jpn. J. Appl. Phys., Part 1* **30**, 1924 (1991).
- ¹⁶R. Langer, A. Barski, J. Simon, N. T. Pelekanos, O. Kononov, R. André, and L. S. Dang, *Appl. Phys. Lett.* **74**, 3610 (1999).
- ¹⁷J. Gleize, F. Demangeot, J. Frandon, M. A. Renucci, F. Widmann, and B. Daudin, *Appl. Phys. Lett.* **74**, 703 (1999).
- ¹⁸M. Schubert, A. Kasic, T. E. Tiwald, J. A. Woollam, V. Härle, and F. Scholz, *MRS Internet J. Nitride Semicond. Res.* **5S1**, W11.39 (2000).
- ¹⁹J. W. Matthews and A. E. Blakeslee, *J. Cryst. Growth* **27**, 118 (1974).
- ²⁰B. Jähnen, M. Albrecht, W. Dorsch, S. Christiansen, H. P. Strunk, D. Hanser, and R. F. Davis, *MRS Internet J. Nitride Semicond. Res.* **3**, 39 (1998).
- ²¹S. J. Hearne, J. Han, S. R. Lee, J. A. Floro, D. M. Follstaedt, E. Chason, and I. S. T. Tsong, *Appl. Phys. Lett.* **76**, 1534 (2000).
- ²²A. Atkinson, T. Johnson, A. H. Harker, and S. C. Jain, *Thin Solid Films* **274**, 106 (1996).
- ²³B. Gil, *Group III Nitride Semiconductor Compounds* (Oxford University Press, Oxford, 1998).
- ²⁴W. Rieger, T. Metzger, H. Angerer, R. Dimitrov, O. Ambacher, and M. Stutzmann, *Appl. Phys. Lett.* **68**, 970 (1996).
- ²⁵S. Chichibu, A. Shikanai, T. Azuhata, T. Sota, A. Kuramata, K. Horino, and S. Nakamura, *Appl. Phys. Lett.* **68**, 3766 (1996).
- ²⁶W. Shan, R. J. Hauenstein, A. J. Fischer, J. J. Song, W. G. Perry, M. D. Bremser, R. F. Davis, and B. Goldenberg, *Phys. Rev. B* **54**, 13460 (1996).

- ²⁷A. Shikanai, T. Azuhata, T. Sota, S. Chichibu, A. Kuramata, K. Horino, and S. Nakamura, J. Appl. Phys. **81**, 417 (1997).
- ²⁸V. Yu. Davydov, N. S. Averkiev, I. N. Goncharuk, D. K. Nelson, I. P. Nikitina, A. S. Polkovnikov, A. N. Smirnov, and M. A. Jacobson, J. Appl. Phys. **82**, 5097 (1997).
- ²⁹I. Lee, I. Choi, C. R. Lee, and S. K. Noh, Appl. Phys. Lett. **71**, 1359 (1997).
- ³⁰A. Cremades, L. Görgens, O. Ambacher, M. Stutzmann, and F. Scholz, Phys. Rev. B **61**, 2812 (2000).
- ³¹S. Nakamura, M. Senoh, S. Nagahama, N. Iwasa, T. Yamada, T. Matsushita, Y. Sugimoto, and H. Kiyoku, Jpn. J. Appl. Phys., Part 2 **36**, L1059 (1997).
- ³²H. Ishikawa, N. Nakada, G. Y. Zhao, T. Egawa, T. Jimbo, and M. Umeno, in *Proceedings of the 2nd International Symposium on Blue Laser and Light Emitting Diodes*, edited by K. Onabe, K. Hiramatsu, K. Itaya, and Y. Nakano (Ohmsha, Tokyo, 1998), p. 727.
- ³³T. Someya, and Y. Arakawa, Appl. Phys. Lett. **73**, 3653 (1998).
- ³⁴J. L. Beuth, Jr., Int. J. Solids Struct. **29**, 1657 (1992).
- ³⁵J. M. Redwing, D. A. S. Loeber, N. G. Anderson, M. A. Tischler, and J. S. Flynn, Appl. Phys. Lett. **69**, 1 (1996).
- ³⁶J. W. Hutchinson, and Z. Suo, in *Advances in Applied Mechanics*, edited by J. W. Hutchinson and T. Wuo (Academic, New York, 1992), Vol. 29, p. 63.
- ³⁷P. Kung, X. Zhang, A. Saxler, D. Walker, M. Razeghi, W. Qian, and V. P. Dravid, J. Eur. Ceram. Soc. **17**, 1781 (1997).